COMMUNICATION

Lanthanide doped upconverting colloidal CaF₂ nanoparticles prepared by a single-step hydrothermal method: toward efficient materials with near infrared-to-near infrared upconversion emission†

Marco Pedroni,[a] Fabio Piccinelli,[a] Tiziana Passuello,[a] Marco Giarola,[b] Gino Mariotto,[b] Stefano Polizzi,[c] Marco Bettinelli[a] and Adolfo Speghini*[a]

Colloidal Er³⁺/Yb³⁺, Tm³⁺/Yb³⁺ and Ho³⁺/Yb³⁺ doped CaF₂ nanoparticles have been prepared by a one-pot hydrothermal procedure and their upconversion properties have been investigated.

Significant efforts have been invested in recent years in order to obtain efficient luminescent materials useful as optical labels in numerous technological applications.[1] Among these materials, lanthanide (Ln) ions doped in suitable inorganic hosts (*e.g.* oxide or fluoride) are excellent for their ability to produce upconversion (UC) emission, *e.g.* emission at higher energy with respect to the exciting radiation.

Of paramount importance is the near infrared (NIR) to red or NIR to NIR UC emission,[2] in which the excitation radiation has a wavelength typically around 1000 nm. This case is particularly important for biomedical purposes. In fact, an excitation in the NIR region coupled with emission also in the NIR (or in the red) is very advantageous, due to the high transparency of the biological fluids in this region, together with a low damage of the tissues[3] and an almost total absence of autofluorescence. Furthermore, upconverting Ln³⁺ doped inorganic nanoparticles (NPs) have many desirable properties, such as high luminescence quantum efficiencies, long lifetimes of the excited states and high photostability.[4]

A highly desirable property of the NPs for many technological applications is a good dispersibility in solvents. This property is strictly correlated to a good separation between the NPs and can be achieved in many cases by capping them with a suitable agent, making them dispersible in the solvent medium. The resulting colloidal dispersions can be easily used in many important applications, such as energy converters in photovoltaic systems[5] or as reporters in biomedical applications.[6] Very interesting upconverting

nanocrystalline materials recently investigated are Er³⁺/Yb³⁺ or Ho³⁺/Yb³⁺ codoped sodium-based fluoride hosts, such as NaYF₄ and NaGdF₄. In fact, these materials have been recently demonstrated to be among the strongest upconverters, and can be easily dispersed in apolar (*e.g.* toluene) and polar (*e.g.* water) solvents, if properly capped with hydrophobic or hydrophilic coordinating organic molecules, respectively.[7] In particular, Er³⁺/Yb³⁺ doped NaYF₄ nanocrystals have been demonstrated to be very interesting as luminescent labels for *in vitro* diagnostic applications.[8]

Undoped and Tb³⁺ doped alkaline-earth fluorides (MF₂, M = Ca, Sr or Ba) have been prepared in colloidal form by thermal decomposition of alkaline-earth trifluoroacetates using oleylamine as a capping agent.[9] A solvothermal technique using ethanol as a solvent was also adopted by Zhang *et al.* to prepare undoped MF₂ (M = Ca, Sr, Ba).[10] From a biological point of view, it is worth noting that calcium fluoride is a very interesting host, as calcium is a non toxic element. Moreover, the Ca²⁺ ion can be easily substituted by a trivalent lanthanide ion, due to similarity in ionic radius;[11] even if charge compensation is necessary to balance the overall ionic charge, the compensation can be achieved by defect formation.[12]

Very recently, Yb³⁺/Er³⁺ codoped CaF₂ NPs grown by a - solvothermal method, by Wang *et al.*,[13] raised attention for their intense UC emission, even stronger than observed for Yb³⁺/Er³⁺ codoped NaYF₄. On the other hand, X-ray diffraction revealed the presence of NaF as an impurity in the synthesized sample, and therefore further efforts should be spent in order to improve the synthetic method. Furthermore, Chen *et al.*[14] prepared Yb³⁺/Tm³⁺ doped SrF₂ NPs by solvothermal synthesis using HF as fluorine precursor. The obtained NPs showed a bright UC luminescence, with a blue emission dominating the spectrum. In both cases, the preparation method produced upconverting NPs surrounded by an oleic acid layer, which allows for good dispersion in apolar solvents (*e.g.* cyclohexane). On the other hand, a second functionalizing step (Lemieux-von Rudloff oxidation) is necessary to convert the capping oleic acid chains to double carboxylic azelaic acid in order to prepare water dispersible MF₂ (M = Ca, Sr) NPs. Moreover, a synthetic method not including the use of toxic HF is desirable for the preparation of fluoride based compounds.

In the present work, we prepared, by a facile, fast and single-step hydrothermal method using water as a solvent, single phase

[a]Laboratorio di Chimica dello Stato Solido, Dipartimento di Biotecnologie, Università di Verona and INSTM, UdR Verona, Strada Le Grazie 15, I-37134 Verona, Italy. E-mail: adolfo.speghini@univr.it; Fax: +39 045 8027929; Tel: +39 045 8027900
[b]Dipartimento di Informatica, Università di Verona, I-37134 Verona, Italy
[c]Dipartimento di Chimica Fisica, Università Ca' Foscari Venezia and INSTM, UdR Venezia, Via Torino 155/b, 30172 Venezia, Mestre, Italy
† Electronic supplementary information (ESI) available. See DOI: 10.1039/c0nr00860e

Yb^{3+}/Tm^{3+}, Yb^{3+}/Ho^{3+} and Yb^{3+}/Er^{3+} co-doped CaF_2 NPs, with strong UC emission upon laser excitation at 980 nm, directly dispersed in the aqueous reaction medium. In particular, upon 980 nm laser excitation, the Tm^{3+}/Yb^{3+} co-doped sample shows a significant emission in the near infrared region around 800 nm.

The preparation procedure of the lanthanide doped CaF_2 NPs (with $Ca^{2+} : Ln^{3+} : Yb^{3+}$ (Ln = Er, Ho or Tm) equal to 0.78 : 0.02 : 0.20 nominal molar ratio) is described in the ESI.† The methodology involves the use of the oleate anion as a capping agent. In order to investigate how the preparation conditions can influence the size and morphology of the NPs, two hydrothermal preparation procedures with different heat treatments have been carried out (at 180 °C for 8 h or at 200 °C for 4 h, see ESI†). After a suitable precipitation technique, the NPs are also directly dispersible in apolar solvents and in water. All the synthesized NPs are shown by X-ray diffraction to be cubic single phases (space group no. 225, $Fm\bar{3}m$), as evidenced by a Rietveld structural and microstructural refinement using the MAUD software[15] on the basis of the crystal structure determined by Laval *et al.* for the $Ca_{0.68}Ln_{0.68}F_{2.32}$ series (Ln= La, Nd, Tb, Ho, Er, Yb, Lu).[16] A representative example for $CaF_2 : Tm^{3+},Yb^{3+}$ NPs prepared after a temperature treatment at 180 °C is shown in Fig. 1. In this structure the presence of clusters of dopant cations, anionic vacancies and interstitial anions has been observed. In fact, as a consequence of the Ca^{2+}/Ln^{3+} substitution, charge compensating mechanisms have to take place. When the Yb^{3+} concentration is higher than 1%, as in the present case, ionic vacancies on the normal F ion site are associated with interstitial fluoride anions in two sites (F′ and F″).[16] The results of the structural Rietveld refinement on CaF_2 doped with 20% Yb^{3+} and 2% Tm^{3+}, prepared after a heat treatment of 180 °C, are shown in Table 1. In addition, for this sample, we obtained an average crystallite dimension of 13(1) nm, in good agreement with the TEM results (see Fig. 1), and 5.473(1) Å as the lattice parameter.

In comparison with undoped CaF_2 (lattice parameter 5.463(1) Å) we observe an increase of the cell volume, probably due to the electronic repulsion between fluoride ions distributed not only in the normal fluoride ion sites but also in interstitial ones, as observed by
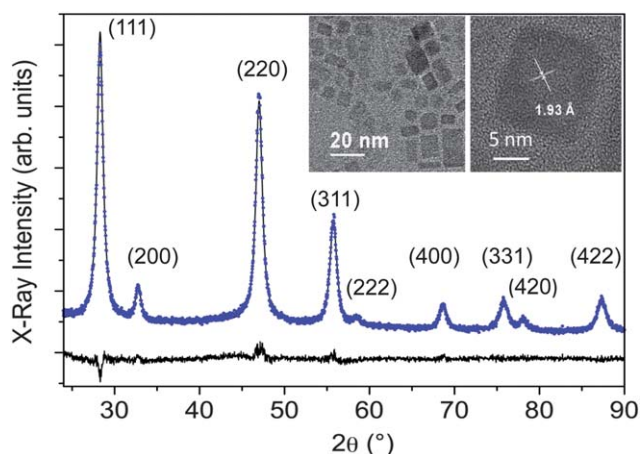
Table 1 Refined structural parameters for the nanocrystalline $CaF_2 : Yb^{3+},Tm^{3+}$ sample prepared after heat treatment at 180 °C

Atom	Site label (atomic coordinates)	Site occupancy	Isotropic thermal factor (B_{iso})
Ca	4a (0,0,0)	0.78(1)	0.60(3)
Yb	4a (0,0,0)	0.20(1)	1.2(3)
Tm	4a (0,0,0)	0.020(1)	1.2(3)
F	8c (1/4, 1/4, 1/4)	0.980(5)	1.54(3)
F′	48i (1/2, x, x), $x = 0.363(5)$	0.00050(7)	0.8(2)
F″	32f (x, x, x), $x = 0.404(9)$	0.025(2)	1.4(5)

Bensalah *et al.*[17] From the Rietveld fit we obtained cell parameters of 5.471(1) Å and 5.469(2) Å, for the Ho^{3+}/Yb^{3+} and Er^{3+}/Yb^{3+} co-doped CaF_2 samples, respectively, while the average crystallite sizes are 22(1) nm and 19(1) nm, respectively (*cf.* ESI†). The presence of the dopant lanthanide ions in the CaF_2 NPs is also confirmed by their EDS spectra (*cf.* ESI†). A representative example is shown in Fig. S4† for the Tm^{3+}/Yb^{3+} co-doped CaF_2 sample, where some peaks attributed to Yb ions are clearly visible. On the other hand, peaks attributed to Tm ions are hardly observed due to their low concentration, which lies below the EDS detection limit. On the other hand, the presence of the Ho^{3+}, Tm^{3+} and Er^{3+} ions is confirmed by their typical emissions, clearly shown in the laser excited upconversion spectra (see Fig. 2). TEM images (see Fig. 1 and S2, ESI†) show that the CaF_2 doped NPs prepared after a heat treatment at 180 C have a quasi regular cubic shape with a slightly broad distribution of sizes and aspect ratios. In particular, the smaller edge of most of the particles is mainly in the range between 7 and 17 nm and the aspect ratio is mainly around 1, even if values around 2 and 3 are observed, as shown in Fig. S3 (*cf.* ESI†). Particles tend to auto-assemble into regular agglomerates with their edges parallel one to the other, but do not show any sintering process, maintaining a short distance of about 1 nm between them. Each particle is a well-grown single crystal, as shown in the inset of Fig. 1.

A different preparation procedure, involving a heat treatment of the starting mixture at 200 °C for 4 h (see ESI†) produces CaF_2 NPs with a much more regular cubic shape and narrow size dispersion with respect to those prepared after a 180 °C. Fig. 2 shows the TEM image and the size distribution plot of these NPs. In particular, it is
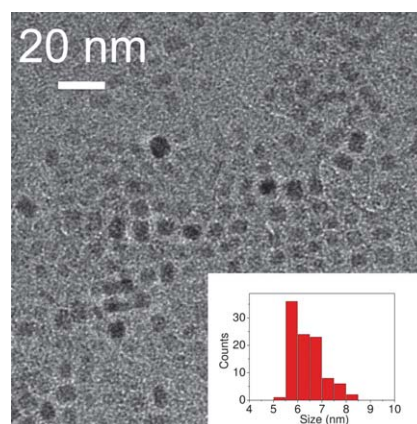

Fig. 1 X-Ray diffraction patterns (blue dots), Rietveld refinement (black solid line) and residuals (lower black line) for $CaF_2 : Tm^{3+},Yb^{3+}$ nanoparticles prepared after heat treatment at 180 °C. Inset: transmission electron microscope (TEM) images for the CaF_2 nanoparticles. The HRTEM picture clearly shows the (220) lattice planes.

Fig. 2 Transmission electron microscope (TEM) image for CaF_2 nanoparticles prepared after a heat treatment at 200 °C for 4 h. Inset: size dispersion of the nanoparticles.

worth noting that the particle size dispersion is less than 2 nm and therefore almost mono-dispersed CaF_2 NPs can be obtained with a careful selection of the preparation conditions.

Fourier transform infrared (FTIR) spectra carried out on pure oleic acid, sodium oleate and oleate capped CaF_2 NPs separated by precipitation clearly indicate that the carboxylate group of the oleate molecule is coordinating the metal on the surface NP (see Fig. 3 and Table S1, ESI†). In fact, the absorption bands at 1561 and 1405 cm^{-1} (assigned to antisymmetric and symmetric carboxylate stretching vibrations[18]) are observed for both sodium oleate and for the oleate capped NPs. On the other hand, the band at 1710 cm^{-1} (assigned to the C=O stretching[19]), which is strong for the oleic acid, almost disappears for the capped CaF_2 NPs, indicating that a small amount of oleic acid is present, presumably dispersed in the oleate capping layer, as found for oleate capped magnetite[20] and YVO_4[21] NPs. Fig. 3 shows the bright luminescence of the prepared $CaF_2 : Ln^{3+}/Yb^{3+}$ (at 180 °C) dispersed in $CHCl_3$ upon 980 nm excitation. The spectra show bands due to the Ln^{3+} ion transitions. All the assignments of the Ln^{3+} emission bands are reported in the caption of Fig. 3. It is worth noting that for the Er^{3+} doped sample, bands in the green, red and NIR regions are observed, even if the red band dominates the spectrum. In fact, the visible luminescence appears yellow to the naked eye (Fig. 3a, inset). Four emission bands are observed for the Ho^{3+} doped sample. Bands of almost the same intensity are observed in the green (510–550 nm) and red (630–660 nm) regions. A medium intensity band in NIR is observed between 730 and 760 nm region while a very weak band is observed between 470 and 480 nm. The green component is stronger than for the Er^{3+} doped sample and the luminescence is mainly green to the

naked eye (see inset of Fig. 3b). The spectrum of the Tm^{3+} doped sample shows a strong emission band at 800 nm (due to the $^3H_4 \rightarrow$ $^3H_6$ transition). The spectrum shows four additional weak bands in the visible region: two in the blue region (450–460 and 460–490 nm) and two in the red region (630–670 and 670–720 nm). It is important to mention that the strong upconversion emission observed for the present lanthanide doped CaF_2 NPs can be explained considering clusterization of the lanthanide ions in the CaF_2 lattice. This phenomenon has been experimentally investigated by Boulon et al. for Yb^{3+} doped Czochralski grown CaF_2 single crystals.[12] This clustering behavior would enhance the probability that each emitting lanthanide ion (Er^{3+}, Ho^{3+} and Tm^{3+}) is in close proximity to Yb^{3+} neighbors with respect to the one based on a statistical distribution of the dopant ions.[22]

The power studies of the colloidal solutions, in which the UC emission intensities are plotted against the laser power densities (shown in Fig. 4 for the three doped samples), demonstrated that more than one photon is involved in the UC process, even if the slopes of the curves in some cases deviate slightly from integer values.[23] It is worth pointing out that the doped CaF_2 NPs obtained after a heat treatment of 200 °C for 4 h show practically identical upconversion spectra with respect to the samples prepared at 180 °C and therefore they are not shown for the sake of simplicity. The mechanisms responsible for the UC luminescence for the Er^{3+}/Yb^{3+},
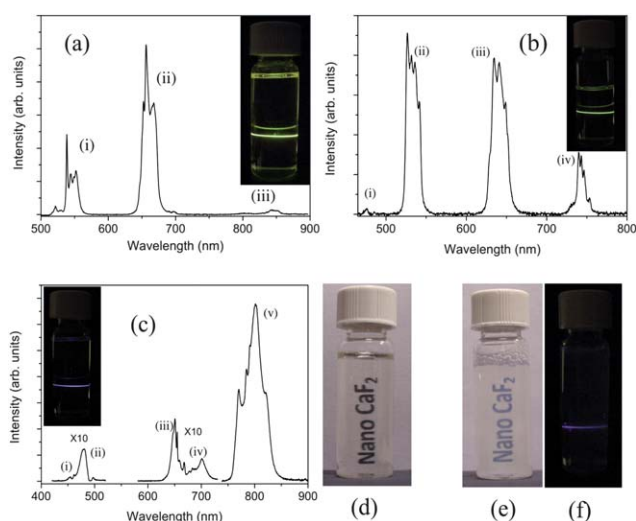

Fig. 3 UC emission spectra ($\lambda_{exc} = 980$ nm) of colloidal solutions (1% wt in $CHCl_3$) of CaF_2 nanoparticles prepared after heat treatment at 180 °C, doped with: (a) Er^{3+}/Yb^{3+} [Er^{3+} transitions: (i) $(^2H_{11/2}, ^4S_{3/2}) \rightarrow ^4I_{15/2}$; (ii) $^4F_{9/2} \rightarrow ^4I_{15/2}$; (iii) $(^2H_{11/2}, ^4S_{3/2}) \rightarrow ^4I_{13/2}$]; (b) Ho^{3+}/Yb^{3+} [Ho^{3+} transitions: (i) $^5F_3 \rightarrow ^5I_8$; (ii) $(^5F_4, \rightarrow ^5S_2) ^5I_8$; (iii) $^5F_5 \rightarrow ^5I_8$; (iv) $(^5F_4, ^5S_2) \rightarrow ^5I_7$]; (c) Tm^{3+}/Yb^{3+} [Tm^{3+} transitions: (i) $^1D_2 \rightarrow ^3F_4$; (ii) $^1G_4 \rightarrow ^3H_6$; (iii) $^1G_4 \rightarrow ^3F_4$; (iv) $^3F_{2,3} \rightarrow ^3H_6$; (v) $^3H_4 \rightarrow ^3H_6$]. Insets of (a), (b), (c): colloidal dispersions showing the UC emission upon 980 nm diode laser excitation. (d) and (e): dispersions of $CaF_2 : Tm^{3+}/Yb^{3+}$ in $CHCl_3$ and water, respectively. (f) UC emission of water colloidal dispersion of $CaF_2 : Tm^{3+}/Yb^{3+}$ nanoparticles observed upon 980 nm laser excitation.
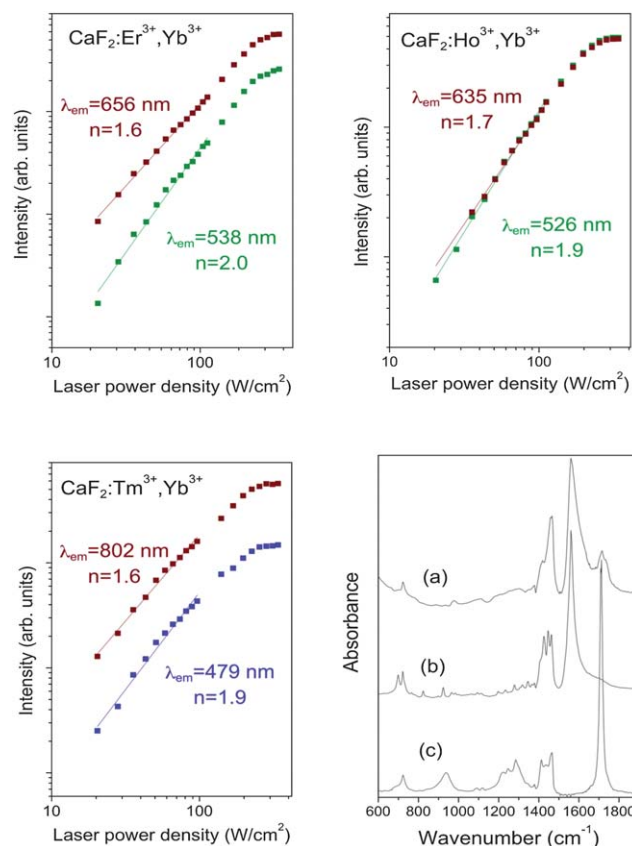

Fig. 4 Power studies for the lanthanide doped CaF_2 nanoparticles prepared after heat treatment at 180 °C ($\lambda_{exc} = 980$ nm). Right lower picture: FTIR absorption spectra of (a) oleate capped CaF_2 nanoparticles obtained after the precipitation procedure, (b) pure sodium oleate, (c) pure oleic acid.

Ho^{3+}/Yb^{3+} and Tm^{3+}/Yb^{3+} co-doped systems are shown in Fig. S5 (*cf.* ESI†).

All the power studies show a saturation behavior at excitation power densities higher than 300 W cm^{-2}. This is a well known behavior commonly found for realistic upconversion systems under large pump absorption.[23] A saturation behavior has also been found for other upconverting fluoride[4] hosts. The knowledge of the power density value for which saturation begins is of valuable importance for practical applications. In fact, it is a useful indication of the upper limit for the excitation radiation power as higher ones are not useful for increasing the upconversion signal. It is also worth underlining that upconverting NPs can increase the spatial resolution in fluorescence diffuse imaging, as recently reported by Svenmarker et al.[24] and Maestro et al.[25] Moreover, the UC emissions are easily measurable for excitation power densities as low as 20 W cm^{-2} (see Fig. 4). This is quite a significant result, also in agreement with the results obtained by Chen et al.,[14] evidencing that the present oleate-capped CaF$_2$ NPs can be employed as efficient upconverting materials in colloidal solutions.

We point out that the supernatant aqueous dispersion obtained after the preparation procedure is almost transparent, and UC emission is clearly visible upon excitation with a 980 nm diode laser (see Fig. 3e and 3f). In this aqueous dispersion, the CaF$_2$ NPs are presumably coated with an oleate double layer, forming a hydrophilic external layer that makes the NPs soluble in water, following the results by Tombàcz et al.[20] In order to strengthen the hypothesis of an oleate double layer formation around the water dispersed CaF$_2$ NPs, we carried out a phase extraction from a CHCl$_3$ colloidal dispersion to an aqueous solution of sodium oleate. As shown in Fig. S6 (*cf.* ESI†) the aqueous layer (upper part) is perfectly transparent and a bright UC emission for the Er^{3+}/Yb^{3+} doped CaF$_2$ sample is clearly visible. This behavior confirms the extraction of the NPs from hydrophobic (CHCl$_3$) to hydrophilic (water) solvents as a consequence of a reorganization of the oleate-capping layer around the NPs. Moreover, zeta potential measurements were performed on water dispersion of the doped NPs (see ESI† for experimental details). All the samples exhibit a negative zeta potential of -62 ± 7 mV. These results indicate that negative charges, mainly due to COO$^-$ groups, are present on the surface of the NPs, in agreement with the results obtained on oleate capped magnetite[20] and yttrium vanadate[21] NPs. A scheme of the proposed double layer is shown in Fig. 5. A layer is composed by oleate molecules with carboxylate group coordinated to the NP surface metal sites. A second layer of oleate molecules is formed by non-covalent interactions among the alkyl chains (see Fig. 5), and the negatively charged COO$^-$ groups on the surface are responsible for the good dispersion of the NPs in polar solvents, such as water.

In conclusion, Er^{3+}/Yb^{3+}, Ho^{3+}/Yb^{3+}, Tm^{3+}/Yb^{3+} codoped CaF$_2$ of cubic shape NPs have been prepared by a one-step, facile and environmentally friendly hydrothermal technique. The NPs are easily dispersed in organic solvents as well as in oleate aqueous solutions, without the need for any post-synthesis reaction. An interesting self-assembling of the NPs is observed from the TEM images. Moreover, we have demonstrated that by choosing carefully the preparation conditions, it is possible to obtain almost mono-dispersed CaF$_2$ NPs, with size dispersion less than 2 nm. The colloidal dispersions show strong UC emissions in the visible and near infrared regions. In particular, the Ho^{3+}/Yb^{3+} and Tm^{3+}/Yb^{3+} doped samples show strong emission in the 750–800 nm region upon 980 diode laser excitation. The very strong and broad emission in the NIR region around 800 nm for the Tm^{3+}/Yb^{3+} doped sample suggests that the present material could be considered among the most adequate materials for NIR to NIR upconversion, and of considerable importance in biomedical luminescence applications, such as optical imaging. The measurements of the upconversion quantum efficiencies of the present NPs are currently in progress.

References

1 (*a*) E. M. Chan, C. Xu, A. W. Mao, G. Han, J. S. Owen, B. E. Cohen and D. J. Milliron, *Nano Lett.*, 2010, **10**, 1874–1885; (*b*) S. Zanarini, E. Rampazzo, L. D. Ciana, M. Marcaccio, E. Marzocchi, M. Montalti, F. Paolucci and L. Prodi, *J. Am. Chem. Soc.*, 2009, **131**, 2260–2267.

2 (*a*) L. Q. X. H. Hu, J. Zhou, F. Y. Li, T. Y. Cao and C. H. Huang, *Chem.–Eur. J.*, 2009, **15**, 3577–3584; (*b*) J. C. Boyer, M.-P. Manseau, J. I. Murray and F. C. J. M. van Veggel, *Langmuir*, 2010, **26**, 1157.

3 O. Ehlert, R. Thomann, M. Darbandi and T. Nann, *ACS Nano*, 2008, **2**, 120–124.

4 F. Vetrone, V. Mahalingam and J. Capobianco, *Chem. Mater.*, 2009, **21**, 1847–1851.

5 H. W. Hillhouse and M. C. Beard, *Curr. Opin. Colloid Interface Sci.*, 2009, **14**, 245–259.

6 Y. Cho and R. B. Borgens, *Nanotechnology*, 2008, **19**, 075603.

7 R. Naccache, F. Vetrone, V. Mahalingam, L. A. Cuccia and J. A. Capobianco, *Chem. Mater.*, 2009, **21**, 717.

8 F. Vetrone, R. Naccache, A. J. de la Fuente, F. Sanz-Rodriguez, A. Blazquez-Castro, E. M. Rodriguez, D. Jaque, J. G. Solé and J. A. Capobianco, *Nanoscale*, 2010, **2**, 495.

9 Z. Quan, D. Yang, X. Zhang, H. Lian, X. Liu and J. Lin, *Inorg. Chem.*, 2008, **47**, 9509–9517.

10 X. Zhang, Z. Quan, J. Yang, P. Yang, H. Lian and J. Lin, *Nanotechnology*, 2008, **19**, 075603.

11 R. D. Shannon and C. T. Prewitt, *Acta Crystallogr., Sect. B: Struct. Crystallogr. Cryst. Chem.*, 1969, **25**, 925.

12 M. Ito, C. Goutadier, Y. Guyot, K. Lebbou, T. Fukuda and G. Boulon, *J. Phys.: Condens. Matter*, 2004, **16**, 1501–1521.

13 G. Wang, Q. Peng and Y. Li, *J. Am. Chem. Soc.*, 2009, **131**, 14200–14201.

14 D. Chen, Y. Yu, F. Huang, P. Huang, A. Yang and Y. Wang, *J. Am. Chem. Soc.*, 2010, **132**, 9976–9978.
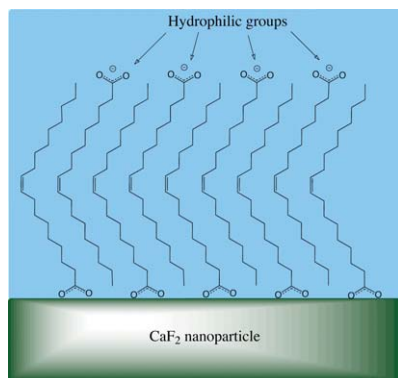
Fig. 5 Scheme of the oleate double layer formed on the CaF$_2$ nanoparticles.

15 L. Lutterotti and S. Gialanella, *Acta Mater.*, 1998, **46**, 101.
16 J. Laval, A. Mikou and B. Frit, *Solid State Ionics*, 1988, **28–30**, 1300–1304.
17 A. Bensalah, M. Mortier, G. Patriarche, P. Gredin and D. Vivine, *J. Solid State Chem.*, 2006, **179**, 2636–2644.
18 (*a*) G. Socrates, *Infrared and Raman Characteristic Group Frequencies* (3rd edn), John Wiley and Sons, Chichester, 2001; (*b*) D. Lin-Vien, N. B. Colthup, W. G. Fateley and J. G. Grasselli, *The Handbook of Infrared and Raman Characteristic Frequencies of Organic Molecules*, Academic Press, San Diego, CA, USA, 1991.
19 J. D. Gelder, K. D. Gussem, P. Vandenabeele and L. Moens, *J. Raman Spectrosc.*, 2007, **38**, 1133–1147.
20 E. Tombácz, D. Bica, E. Illes, A. Majzik and L. Vekas, *J. Phys.: Condens. Matter*, 2008, **20**, 204103.

21 T. Taniguchi, T. Watanabe, K. Katsumata, K. Okada and N. Matsushita, *J. Phys. Chem. C*, 2010, **114**, 3763–3769.
22 B. M. van der Ende, L. Aarts and A. Meijerink, *Adv. Mater.*, 2009, **21**, 3073–3077.
23 M. Pollnau, D. R. Gamelin, S. R. Lüthi, H. U. Güdel and M. P. Helhlen, *Phys. Rev. B: Condens. Matter Mater. Phys.*, 2000, **61**, 3337–3346.
24 P. Svenmaker, C. T. Xu and S. Andersson-Engels, *Opt. Lett.*, 2010, **35**, 2789–2791.
25 L. M. Maestro, E. M. Rodriguez, F. Vetrone, R. Naccache, H. L. Ramirez, D. Jaque, J. A. Capobianco and J. G. Solé, *Opt. Express*, 2010, **18**, 23544–23553.